IEICE TRANS. ELECTRON., VOL.E99–C, NO.6 JUNE 2016

INVITED PAPER *Special Section on Cutting-Edge Technologies of Superconducting Electronics*

Development of an Advanced Circuit Model for Superconducting Strip Line Detector Arrays

Ali BOZBEY[†,††a)], **Yuma KITA**[††], **Kyohei KAMIYA**[††], ***Nonmembers***, **Misaki KOZAKA**[††], **Masamitsu TANAKA**[††], ***Members***, **Takekazu ISHIDA**[†††], ***Nonmember***, ***and*** **Akira FUJIMAKI**[††], ***Member***

SUMMARY One of the fundamental problems in many-pixel detectors implemented in cryogenics environments is the number of bias and read-out wires. If one targets a megapixel range detector, number of wires should be significantly reduced. One possibility is that the detectors are serially connected and biased by using only one line and read-out is accomplished by on-chip circuitry. In addition to the number of pixels, the detectors should have fast response times, low dead times, high sensitivities, low inter-pixel crosstalk and ability to respond to simultaneous irradiations to individual pixels for practical purposes. We have developed an equivalent circuit model for a serially connected superconducting strip line detector (SSLD) array together with the read-out electronics. In the model we take into account the capacitive effects due to the ground plane under the detector, effects of the shunt resistors fabricated under the SSLD layer, low pass filters placed between the individual pixels that enable individual operation of each pixel and series resistors that prevents the DC bias current flowing to the read-out electronics as well as adjust the time constants of the inductive SSLD loop. We explain the results of investigation of the following parameters: Crosstalk between the neighbor pixels, response to simultaneous irradiation, dead times, L/R time constants, low pass filters, and integration with the SFQ front-end circuit. Based on the simulation results, we show that SSLDs are promising devices for detecting a wide range of incident radiation such as neurons, X-rays and THz waves in many-pixel configurations.

key words: *SSLD, kinetic inductance detectors, SFQ, superconductors, neutron detector*

1. Introduction

Superconducting stripline detectors are promising devices especially for many-pixel applications up to megapixel [1] resolutions when combined with single flux quantum (SFQ) read-out schemes [2]–[4]. It is possible to use only one bias point for an SSLD array and fabricate the detector together with the SFQ read-out electronics on the same chip in a monolithic configuration. Proof of concept devices have already been demonstrated [5], [6] and a feasibility for the megapixel scaling have been reported [1]. In addition, a recent study reports the electrothermal model for these devices [7]. As the performance parameters such as sensitivity, response time, and spatial resolution heavily depend on the physical and electrical parameters of the device, it is needed to create an equivalent circuit model which is suitable for engineering the devices. In this paper, the input patterns for the simulation are based on a fiber coupled laser of the wavelength of 1550 nm which is used for the proof of concept experiments at the laboratory. However, SSLDs have the potential of being used for detecting photons and particles in a wide range of spectrum. For instance, if proper absorbing layers are deposited on top of the SSLDs, they can be used as a Neutron or X-ray detectors. If suitable antennas are coupled to individual SSLDs, THz imaging arrays can be fabricated.

One other important aspect of the SSLDs is that they have two modes of operation. Namely, inductive mode of operation and resistive mode of operation. If the SSLD is remains in the superconducting state response is generated based on current biased kinetic inductance detector principles [5]. However, if the incident radiation forces part of the SSLD to normal state, then the response is generated based on bolometric [8] or superconducting nanowire single-photon detector [9] operation principles. Here we report the details of the model and simulation results that we have obtained for both modes of operation for various configurations.

2. Model Details

2.1 Detector Configuration and Circuit Model

One pixel of an SSLD is composed of a superconducting stripline, a series resistance to the stripline, and a coupling coil. Stripline is the sensitive part of the detector, series resistance adjusts the time constant of the device as well as it converts the voltage signal to current, and coupling coil transfers the detector response to the read-out circuit. In the array configuration, low pass filters of the gain of about −3 dB at a frequency of 100 MHz are placed between pixels so that response generated at one SSLD does not propagate to neighbor SSLDs. This configuration is already reported elsewhere [1] and in Fig. 1 we report the proposed circuit model for that configuration. Each SSLD is a meander line with 0.7 μm width, 50 nm thickness and 2 cm length. Distance of the SSLD layer from the ground plane is 740 nm.

We have created a circuit model for 500 serially connected SSLDs for the configuration reported in [1] as shown in Fig. 1. In the figure, L_1 is the irradiated part of the stripline where the voltage is generated according to the re-

Manuscript received October 20, 2015.
Manuscript revised January 6, 2016.

[†]The author is with TOBB University of Economics and Technology, 06560, Ankara, Turkey.
[††]The authors are with Nagoya University, Nagoya-shi, 464–8603 Japan.
[†††]The author is with Osaka Prefecture University, Sakai-shi, 599–8531 Japan.
a) E-mail: bozbey@etu.edu.tr

DOI: 10.1587/transele.E99.C.676

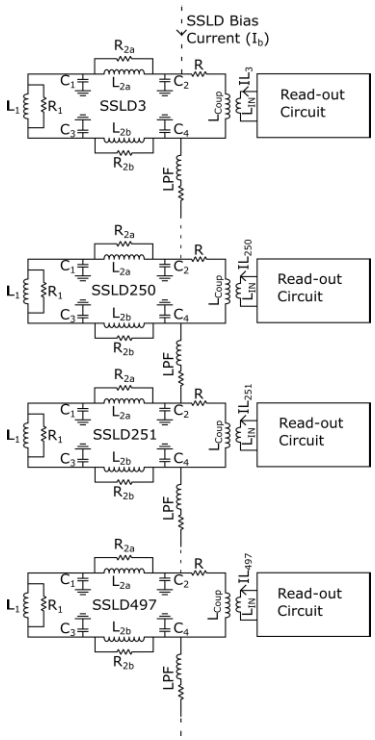

Fig. 1 SSLD array configuration and circuit model. L_1 is the irradiated part of the stripline, L_{2a} and L_{2b} represent the part of the SSLD where no radiation is exposed, C_1-C_4 are the parasitic capacitance of the SSLDs, R_{2a} and R_{2b} model the shunt resistances that are fabricated under the SSLDs. L_{COUP} and L_{IN} represent the coupling coil to transfer the SSLD current to read-out circuit. LPF is a series L-R low pass filter circuit to prevent the crosstalk between pixels. IL_3-IL_{497} represent the coupled current to the read-out circuit.

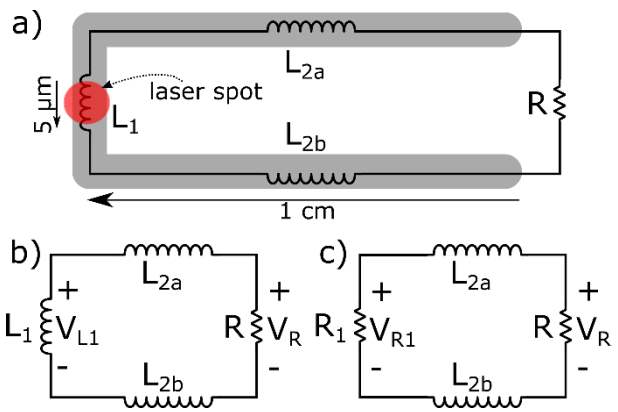

Fig. 2 (a) Simplified circuit model of the SSLD that shows the sources of L1 and L2 in the model. In this configuration, irradiation is assumed to be at the center and $L_{2a} = L_{2b}$. (b) shows the inductive mode and (c) shows the resistive mode models.

lation shown in Eq. (1) or Eq. (2) depending on the mode of operation. $L_2 = L_{2a} + L_{2b}$ represents the part of the SSLD where no radiation is exposed. L_1 value is determined by the spot size of the laser, which is a circle of about 5 μm diameter as shown in Fig. 2 (a). As the total length of the SSLD is 2 cm, L_2/L_1 is about 4000. L_{2a}/L_{2b} ratio is determined by the location of the irradiation on the SSLD.

Different from similar models developed for superconducting nanowire single photon detectors (SNSPD) [10], [11] we have taken into account the parasitic capacitance of the SSLDs (C_1-C_4) as the physical dimensions of the detectors are large and they have a ground plane underneath. The reason for using a ground plane under the SSLDs is that as the dimensions of the stripline are in the order of cm, transmission-like behavior is needed to enable pulse propagation over the SSLD. Total capacitance of the SSLD is calculated as 1.950 pF and this value is distributed among C_1-C_4 in proportional with the L_{2a}/L_{2b} ratio during the simulations. In Sects. 3.1–3.4, where $L_{2a}/L_{2b} = 1$, $C_1 = C_3 = 0.325$ pF and $C_2 = C_4 = 0.650$ pF values are used. For the calculations in Sect. 3.5, where $L_{2a}/L_{2b} = 100$, capacitance values are scaled accordingly.

In addition, the shunt resistances R_{2a} and R_{2b} model the resistances that are fabricated under the SSLDs to decrease the quality factor of the stripline configuration and dampen any possible oscillation in the loop.

Figure 2 shows the simplified models of the SSLD for inductive and resistive modes of operation. Generated responses V_{L1} and V_{R1} due to incoming radiation for each mode are shown in Eqs. (1) and (2).

$$V_{L1}(t) = I_B \times \frac{dL_1(t)}{dt} \tag{1}$$

$$V_{R1}(t) = I_B \times R_1(t) \tag{2}$$

Where, I_B represents the DC bias current of the SSLD, $L_1(t)$ represents the change of the kinetic inductance of the SSLD due to the irradiation, and $R_1(t)$ represents the generated resistance of the irradiated part of the SSLD due to local heating. In both modes of operation, the generated voltage is converted to current by the series resistance R and coupled to the read-out circuit by the coupling coil as shown in Fig. 1. In the simulation, we monitor the current at the secondary side of the coil (L_{IN}) which is directly connected to the read-out circuit shown in Fig. 4.

In order to determine the voltage input characteristics of the SSLD that simulate the actual response, we solved the simple model shown in Fig. 2 analytically in Laplace domain. For various inductance transients, voltage characteristics are obtained as shown in Fig. 3. Throughout the paper, for inductive mode, we use the fastest input signal shown in Fig. 3 (b) that corresponds to 0.1 ns rise/fall times of inductance transient in order to show that the SSLDs can respond to such fast signals. For the positive side of V_R, we see that the voltage can track the inductance transient whereas for the negative side, recovery time is much slower. This value corresponds to the L_2/R time constant of the loop, which is 10 nH/5 Ω = 2 ns.

2.2 Read-Out Circuit

Response of each SSLD pixel is transferred to the read-out electronics by using the coupling coil shown in Fig. 1. Read-out circuit may be composed of a SQUID or quasi-one

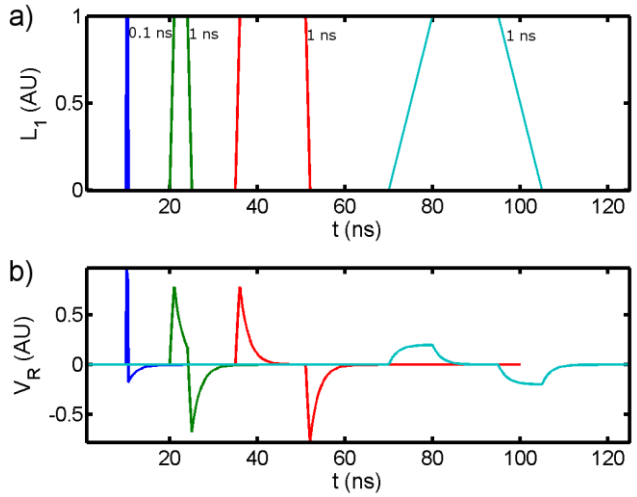

Fig. 3 Generated voltage at the resistor of Fig. 2 (a) for various inductance transients for inductive mode. The result is based on a standard transfer function solution in the Laplace domain. Rise times of the L_1 transients are 0.1 ns, 1 ns, 1 ns, 10 ns respectively. For the simulation we used L_2 = 10 nH and R = 5 Ω.

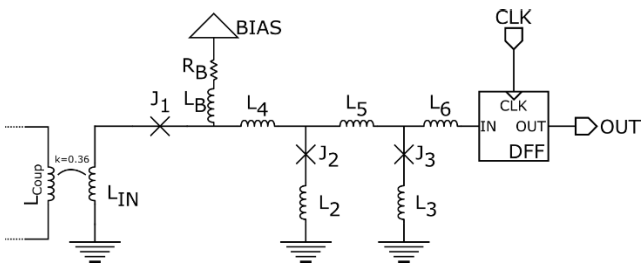

Fig. 4 Read-out circuit for one SSLD pixel. I_{J1} = 70 μA, I_{J1} = 110 μA, I_{J1} = 155 μA, L_{IN} = 9.4 pH, L_5 = 6.7 pH, L_6 = 1.6 pH, L_2, L_3, and L_4 are parasitic inductances. R_B and L_B are the bias resistor and inductors respectively. Left side of the coupling coil belongs to the SSLD. k is the coupling coefficient between L_{IN} and L_{COUP}. CLK is the DFFe clock pulse. QOS is formed by the J_1-L_4-J_2 loop. DFFe cell is used from the CONNECT cell library.

junction SQUID (QOS) [12] that gives a logic "1" output if the coupled current is higher than a predetermined threshold with the arrival of a sampling clock. In the paper we report the simulation results of a QOS based read-out circuit. In this design, different from conventional QOS circuits [12], [13] we utilized a clock-free QOS (CF-QOS) that oscillates with the arrival of a coupled current. At the output of the CF-QOS, a delay flip flop (DFF) circuit is connected so that any single flux quantum (SFQ) pulse that is generated at the CF-QOS is latched. DFFe cell was used from the CONNECT cell library [14] that allows inputting consecutive SFQ pulses before DFFe clock pulse (*CLK*) is triggered as shown in Fig. 4. The reason for using such a configuration is that it simplifies the digital processing circuit but more importantly, the sampling clock may be much lower than the duration of the response especially at the inductive mode of operation. Even if the inductive response duration is much shorter than the clock period, since the SFQ pulse is latched at DFFe, with the arrival of a slower clock output

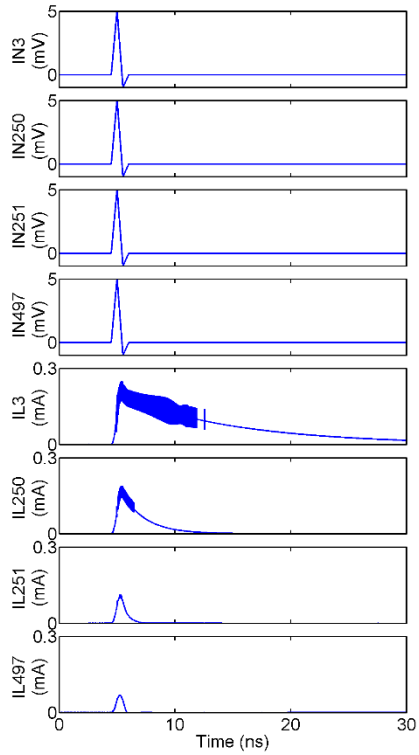

Fig. 5 Effect of the L/R time constant of the SSLD loop under inductive mode of operation. $SSLD_3$-$SSLD_{497}$ have 1, 5, 20, and 50 Ω series resistances respectively.

can be obtained.

2.3 Resistive and Inductive Modes of Operation

SSLDs have two modes of operation, namely, inductive mode and resistive mode. If the SSLD is biased much lower than the critical current of the superconducting stripline or if the incoming radiation energy and/or intensity is low then local heating is not sufficient to have the stripline to switch to normal state. Then the stripline remains in the superconducting state but the kinetic inductance changes due to broken cooper pairs [15]. In this mode of operation, it is assumed that the response at the SSLD is generated due to the change in the kinetic inductance of the detector which generates a voltage signal proportional to dL/dt as shown in Eq. (1). This behavior is previously investigated and named as current biased kinetic inductance detector (CB-KID) [6]. If the SSLD is biased close to the critical current of the stripline, then an incoming radiation causes part of SSLD switch to the normal state and change of resistance translates to a voltage signal under constant bias current with a relation shown in Eq. (2). The characteristics of this mode is similar to a superconducting nanowire single photon detector (SNSPD) [9] or transition edge sensors (TES) [8]. Even though the output characteristics and read-out scheme for both modes of operation are similar, signal durations and shapes are different as shown in Figs. 5 and 6. Details of the inductive mode input has been explained in Sect. 2.1. For

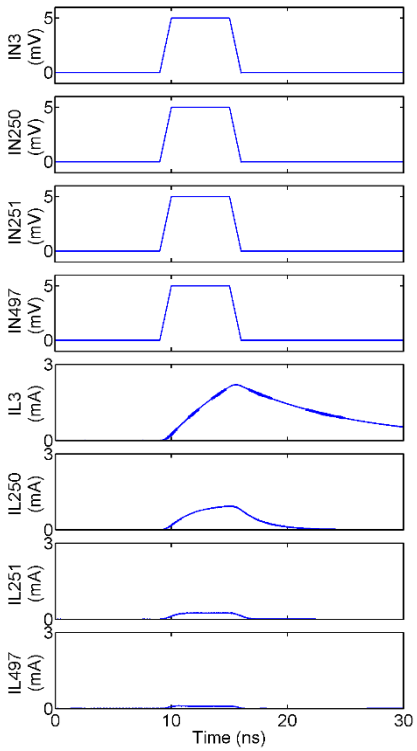

Fig. 6 Effect of the L/R time constant of the SSLD loop under resistive mode of operation. $SSLD_3$-$SSLD_{497}$ have 1, 5, 20, and 50 Ω series resistances respectively.

the resistive mode of operation input pattern, we assume that SSLD tracks the input pulse characteristics of our laser with 1 ns rise/fall times. Hence, inductive response duration is generally much shorter than that of resistive response. One thing to note is that, SSLD biasing or read-out scheme is the same for both modes of operation and it is not critical to force the SSLD array to operate in one mode of operation as long as the timings and signal amplitudes are in acceptable range.

3. Simulation Results

We have simulated the circuit shown in Fig. 1 by exciting four of the SSLD pixels out of 500 and observed the responses of excited pixels as well as neighbor pixels. We used Jsim simulator [16] for all the simulations. In all the simulations, we applied triangular input to simulate inductive mode of operation, similar to the measurement results of [6], and square input to simulate the resistive mode of operation similar to the optical source that we use in our experiments, 1550 nm wavelength laser with 1 ns rise/fall times and 5ns duration time.

3.1 L/R Time Constant of the SSLD Pixel

L/R time constant of the stripline affects the response time and output amplitude of the SSLD directly. To see the effect of the L/R time constant of the SSLD loop, we kept the

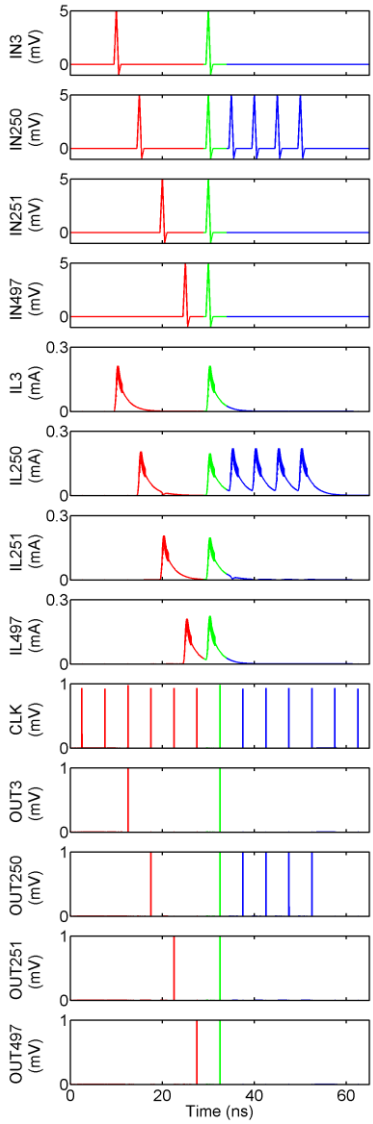

Fig. 7 Demonstration of the crosstalk (0-25ns), simultaneous radiation (30-35ns), and repetition rate (35-65ns) for inductive mode of operation. IN_3, IN_{250}, IN_{251}, and IN_{497} show the input for 3rd, 250th, 251st, and 497th SSLDs. IL_3-IL_{497} show the current in the coupling coil of the SSLD, OUT_3-OUT_{497} show the output of the respective SFQ front-end.

inductance of the stripline as 10 nH and changed the series resistance R from 1 Ω to 50 Ω. As shown in Figs. 5 and 6 we see that as R is increased, response speed of the SSLD increases due to the L/R time constant of the SSLD loop. In this case, the amount of the coupled current (I_{L3}-I_{L497}) decreases due to Ohms's law $I = V/I$. It should be noted that SSLD voltage response is given by (1) or (2), which is constant for a given SSLD and incident radiation. We plan to read-out the response of the SSLDs with a QOS comparator circuit and the coupled current should be greater than the threshold value and gray-zone width of the comparator [12]. For this configuration we considered that best compromise between speed and coupled current magnitude is using R = 5 Ω in terms of speed and coupled current magnitude and used this value for the rest of the simulations.

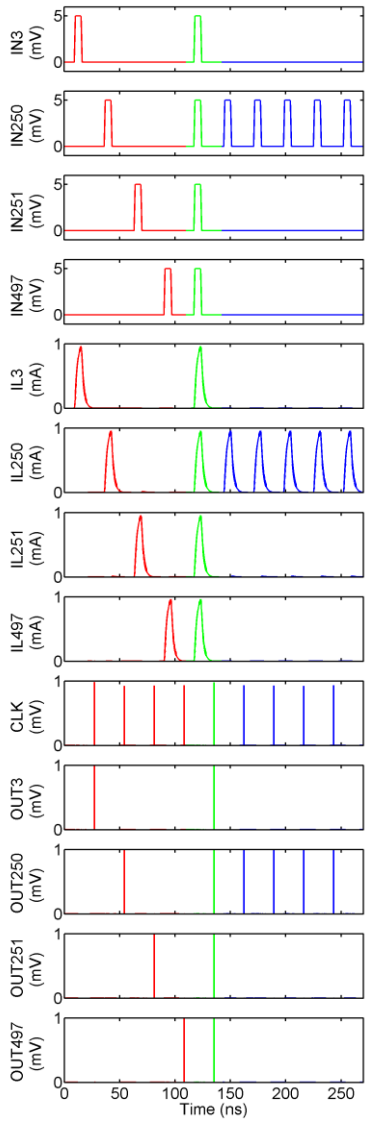

Fig. 8 Demonstration of the crosstalk (0-125ns), simultaneous radiation (130-150 ns), and repetition rate (150-250 ns) for resistive mode of operation. IN_3, IN_{250}, IN_{251}, and IN_{497} show the input for 3rd, 250th, 251st, and 497th SSLDs. IL_3-IL_{497} show the current in the coupling coil of the SSLD, OUT_3-OUT_{497} show the output of the respective SFQ front-end.

3.2 Inter-Pixel Crosstalk

One of the important aspects of a multi-pixel detector configuration is that the radiation falling on one of the pixels should not generate output at the neighbor pixels and read-out circuitry. As we placed low pass filters between the SSLDs, response generated at one of the pixels cannot propagate to the neighbor pixels and all the signal is directed towards the read-out circuit. This is shown in Figs. 7 and 8 in the duration of 0-25 ns and 0-125 ns intervals respectively. In the figures, IN_3-IN_{497} represent the input voltages V_{L1} or V_{R1} of Fig. 2 for SSLD$_3$-SSLD$_{497}$ respectively. As shown in the figures, when the pixels 3, 250, 251, and 497 are irradiated at different times (IN_3-IN_{497}), neither any current is coupled to the coupling coils of other pixels (I_{L3}-I_{L497}) nor is any response generated at the read-out circuit (OUT_3-OUT_{497}). Current is coupled only to the corresponding coil and only that read-out circuit gives output. For instance, when SSLD$_{250}$ is excited, current is coupled to LIN_{250} and SFQ output is generated at OUT_{250} only.

3.3 Response to Simultaneous Radiation

When the pixels are irradiated simultaneously, the response should not be affected from neighbor pixels irradiation. This is important as in an actual system photons can fall onto the pixels randomly and under such circumstances, individual pixels should be able to operate independent from each other. To test this effect we have excited all the pixels at 30 ns for inductive mode and at 140 ns for resistive mode as shown in Figs. 7 and 8 respectively. When we observe the outputs as shown in the figures, coupled current and SFQ outputs operate as expected. From this result we can say that such a configuration is suitable for an imaging application.

3.4 Interval between Inputs and Dead-Time of the SSLD

One of the circuit parameters that affects the maximum repetition rate of the incoming signal is the L/R time constant of the SSLD. As the designed SSLDs have 10 nH inductance and 5 Ω resistance, L/R time constants of the SSLD loops are 2 ns. We have supplied input patterns to 250th SSLD and observed the output. For the inductive mode of operation repetition period is 5 ns and for resistive mode of operation, repetition period is 20 ns as the input pattern duration is already higher than 5 ns. As shown in Figs. 7 and 8 at 30-65 ns and 150-250 ns intervals, coupled current and SFQ output operates correctly at a repetition rate of 5 ns and 20ns respectively.

3.5 Position Dependence of the Radiation at the Stripline

For the simulations in this part, we assumed that irradiation occurs at two edges of the SSLD as shown in Fig. 9. As the laser spot moves on the SSLD, L_{2a}/L_{2b} ratio is changed while $L_{2a} + L_{2b} = L_2$ remains constant. Figure 9 (a) shows the case of $L_{2a}/L_{2b} = 0.01$ and Fig. 9 (b) shows the case of $L_{2a}/L_{2b} = 100$. Figures 10 and 11 show the results for $L_{2a}/L_{2b} = 0.01$ (IN_{250}) and $L_{2a}/L_{2b} = 100$ (IN_{251}) respectively which correspond to irradiations at the two edges of the SSLDs. As shown in Figs. 10 and 11, regardless of the position of illumination SSLD output is as expected. Hence, we can deduce that this configuration is suitable for using the addressing scheme proposed in [1].

4. Conclusion

In this work, we have developed an advanced model to explain and predict different behaviors of superconducting stripline detectors both in inductive and resistive modes of

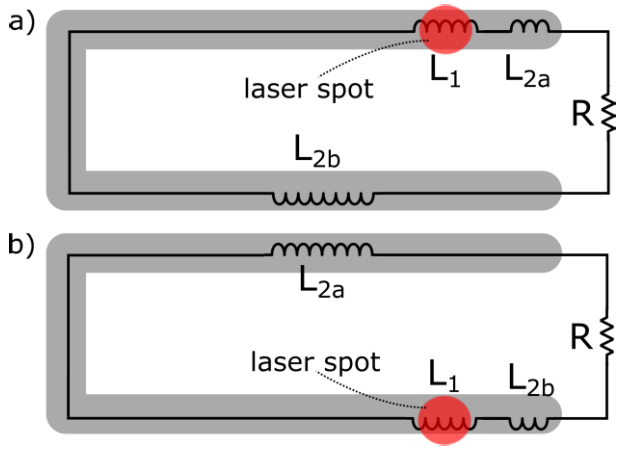

Fig. 9 Illustration of the radiation position effect on the circuit parameters of the model. (a) shows the case of $L_{2a}/L_{2b} = 0.01$ and (b) shows the case of $L_{2a}/L_{2b} = 100$. Figures are not to scale and show only the inductances for simplicity. Shunt resistors and parasitic capacitors of the SSLDs are scaled accordingly during simulation.

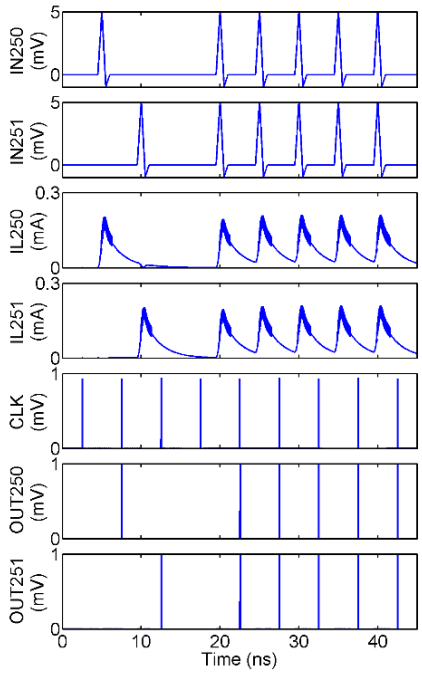

Fig. 10 Effect of the radiation at various positions of the SSLD pixel for the inductive mode of operation. 250th pixel is radiated at the position $L_{2a}/L_{2b} = 0.01$ and 251st pixel is radiated at the position $L_{2a}/L_{2b} = 100$.

operation. We have shown that proposed configuration is suitable for crosstalk-free operation at low dead-times with the capability of single flux quantum logic read-out that will allow us to develop megapixel resolution imaging array. We anticipate that SSLDs have the potential of being used for detecting photons and particles in a wide range of spectrum if proper absorber layer and/or antennas are coupled to the detectors. With the use of advanced models similar to this paper, it will be possible to engineer the device structures for speed, number of pixels, and sensitivity.

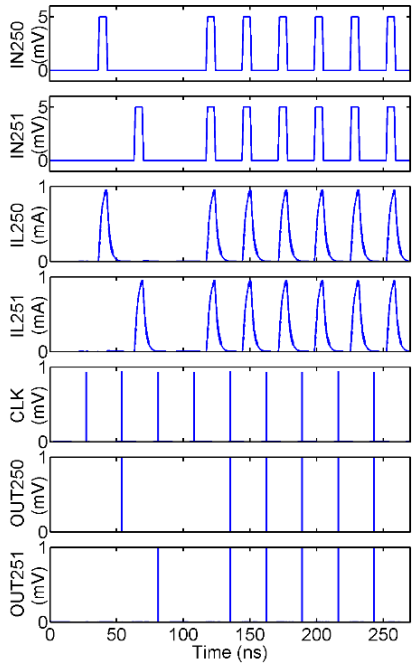

Fig. 11 Effect of the radiation at various positions of the SSLD pixel for the resistive mode of operation. 250th pixel is radiated at the position $L_{2a}/L_{2b} = 0.01$ and 251st pixel is radiated at the position $L_{2a}/L_{2b} = 100$.

Acknowledgments

This work is partially supported by TUBITAK with the project number 114E099 and JSPS KAKENHI with the grant number 23226019.

References

[1] T. Ishida, N. Yoshioka, Y. Narukami, H. Shishido, S. Miyajima, A. Fujimaki, S. Miki, Z. Wang, and M. Hidaka, "Toward mega-pixel neutron imager using current-biased kinetic inductance detectors of Nb nanowires with 10B converter," J. Low Temp. Phys., vol.176, no.3-4, pp.216–221, Aug. 2014.

[2] H. Terai, S. Miki, and Z. Wang, "Readout electronics using single-flux-quantum circuit technology for superconducting single-photon detector array," IEEE Trans. Appl. Supercond., vol.19, no.3, pp.350–353, June 2009.

[3] A. Bozbey, S. Miyajima, H. Akaike, and A. Fujimaki, "Single-flux-quantum circuit based readout system for detector arrays by using time to digital conversion," IEEE Trans. Appl. Supercond., vol.19, no.3, pp.509–513, June 2009.

[4] H. Terai, S. Miki, T. Yamashita, K. Makise, and Z. Wang, "Demonstration of single-flux-quantum readout operation for superconducting single-photon detectors," Appl. Phys. Lett., vol.97, no.11, 112510, Sept. 2010.

[5] N. Yoshioka, Y. Narukami, S. Miyajima, H. Shishido, A. Fujimaki, S. Miki, Z. Wang, and T. Ishida, "Four-channel current-biased kinetic inductance detectors using MgB_2 nanowires for sensing pulsed laser irradiation," J. Low Temp. Phys., vol.173, no.3-4, pp.273–278, 2014.

[6] N. Yoshioka, I. Yagi, H. Shishido, T. Yotsuya, S. Miyajima, A. Fujimaki, S. Miki, Z. Wang, and T. Ishida, "Current-biased kinetic inductance detector using MgB_2 nanowires for detecting neutrons," IEEE Trans. Appl. Supercond., vol.23, no.3, 2400604, June 2013.

[7] C.N. Thomas, S. Withington, and D.J. Goldie, "Electrothermal model of kinetic inductance detectors," Supercond. Sci. Technol., vol.28, no.4, 045012, April 2015.
[8] K.D. Irwin and G.C. Hilton, "Transition-edge sensors," in Cryogenic Particle Detection, C. Enss, ed., Topics in Applied Physics, vol.99, pp.63–150, Springer Berlin Heidelberg, 2005.
[9] C.M. Natarajan, M.G. Tanner, and R.H. Hadfield, "Superconducting nanowire single-photon detectors: Physics and applications," Supercond. Sci. Technol., vol.25, no.6, 063001, June 2012.
[10] S. Jahanmirinejad and A. Fiore, "Proposal for a superconducting photon number resolving detector with large dynamic range," Opt. Express, vol.20, no.5, pp.5017–5028, Feb. 2012.
[11] S. Jahanmirinejad, G. Frucci, F. Mattioli, D. Sahin, A. Gaggero, R. Leoni, and A. Fiore, "Photon-number resolving detector based on a series array of superconducting nanowires," Appl. Phys. Lett., vol.101, no.7, 072602, Aug. 2012.
[12] A. Bozbey, S. Miyajima, T. Ortlepp, and A. Fujimaki, "Design and circuit analysis of quasi-one junction SQUID comparators for low temperature detector array read-out," J. Supercond. Nov. Magn., vol.24, no.1, pp.1065–1069, 2011.
[13] H. Ko and T. van Duzer, "A new high-speed periodic-threshold comparator for use in a Josephson A/D converter," IEEE J. Solid-State Circuits, vol.23, no.4, pp.1017–1021, 1988.
[14] S. Yorozu, Y. Kameda, H. Terai, A. Fujimaki, T. Yamada, and S. Tahara, "A single flux quantum standard logic cell library," Phys. C Supercond., vol.378-381, pp.1471–1474, 2002.
[15] P.K. Day, H.G. LeDuc, B.A. Mazin, A. Vayonakis, and J. Zmuidzinas, "A broadband superconducting detector suitable for use in large arrays," Nature, vol.425, no.6960, pp.817–821, Oct. 2003.
[16] E.S. Fang and T. van Duzer, "A Josephson integrated circuit simulator (JSIM) for superconductive electronics application," Ext. Abstr. 2nd ISEC Tokyo Jpn., pp.407–410, 1989.

Ali Bozbey received the B.S., M.S., and Ph.D. degrees in electrical and electronics engineering from Bilkent University, Ankara, Turkey, in 2001, 2003, and 2006, respectively. In 2002, he was a Guest Researcher with the Jülich Research Center, Jülich, Germany, and in 2007, he was a Postdoctoral Researcher with Nagoya University, Nagoya, Japan. Since 2008, he has been with the Department of Electrical and Electronics Engineering, TOBB University of Economics and Technology, Ankara, Turkey.

Yuma Kita received the B.E. and M.E. from Nagoya University, Nagoya, Japan in 2013 and 2015 respectively. His research interests include superconducting digital circuits and superconducting detectors.

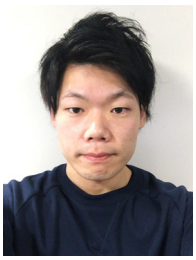

Kyohei Kamiya received the B.E. from Nagoya University, Nagoya, Japan in 2015. His research interests are superconducting detectors and systems.

Misaki Kozaka received the B.E. from Nagoya University, Nagoya, Japan in 2014. His research interests include superconducting digital circuits and applications.

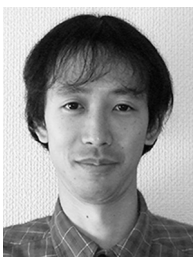

Masamitsu Tanaka received the M.E. and Ph.D. degrees in electronics and information electronics from Nagoya University, Nagoya, Japan, in 2003 and 2006, respectively. He was a JSPS Research Fellow from 2005 to 2007. He joined Department of Information Engineering, Nagoya University in 2007, and moved to Department of Quantum Engineering in 2010, where he is currently a designated lecturer. In 2011 he was a research scholar at the University of California, Berkeley, CA, USA. His research interests include the ultra-fast/energy-efficient computing using RSFQ circuits and logic design methodologies.

Takekazu Ishida received the B.E. from Tohoku University, Sendai, Japan, in 1976. He received the M.E. and Ph.D. degrees from Kyoto University in 1978 and 1982, respectively. He has been working on material properties of superconductors for years. He proposed a new idea to produce a neutron detector using a new superconductor MgB_2 in 2001. He is currently a professor of Department of Physics and Electronics at Osaka Prefecture University. His research interests are nanofabrication of superconductor, its potential application as superconducting devices and magnetic properties of anisotropic superconductors.

Akira Fujimaki received his B.E, M.E., and Dr. Eng. degrees from Tohoku University in 1982, 1984, and 1987, respectively. He was a Visiting Assistant Research Engineer at the University of California, Berkeley, in 1987. Since 1988, he has been working on superconductor devices and circuits at the School of Engineering, Nagoya University, Nagoya, Japan, where he is currently a professor. His current research interests include single-flux-quantum circuits and their applications based on low- and high-temperature superconductors.